iJRASET
International Journal For Research in Applied Science and Engineering Technology

# INTERNATIONAL JOURNAL FOR RESEARCH

IN APPLIED SCIENCE & ENGINEERING TECHNOLOGY

**Volume:** 9 **Issue:** VI **Month of publication:** June 2021

**DOI:** https://doi.org/10.22214/ijraset.2021.35705

www.ijraset.com

Call: 08813907089 | E-mail ID: ijraset@gmail.com

International Journal for Research in Applied Science & Engineering Technology (IJRASET)
*ISSN: 2321-9653; IC Value: 45.98; SJ Impact Factor: 7.429*
*Volume 9 Issue VI Jun 2021- Available at www.ijraset.com*

# Behaviour of Shear Connector in CFST for Axial Strength

Seema Subhash Rathod[1], Dr. S. A. Bhalchandra[2]
[1]*PG Scholar,* [2]*Dr.of Department of Civil Engineering, Government College of Engineering, Aurangabad, India*

***Abstract:*** ***Concrete Filled Steel structures (CFST) offers wide benefits like high strength, ductility, and energy absorption with the combined benefits of steels and concrete. It also reduces the complexity of the production, as it does not require the shuttering of work, and so it is not commonly used. In addition to CFST elements, are more efficient, and allow for rapid construction and cost savings due to the elimination of the shape and material of component part. Concrete-filled-steel-tube is currently gaining more and more popularity in the construction industry. Concrete-filled-steel-tube it is a component of a good performance, as a result of the impact of the steel and holds it with concrete, and the question of structural diversity. In this paper, it presents a study of the evolution of the load carrying capacity, used for the connection of a variety of sizes and shapes, with a different position. The composite action of steel and concrete there is a need for a strong bond between the steel and concrete interface. Analysis of CFST column using the Finite element method and the numerical study is done on the selected case under axial loading condition.***

***Keywords: CFST Column, Stiffener, ABAQUS software***

## I. INTRODUCTION

Steel components have the advantages of high tensile strength, and yield strength, while the concrete elements have the advantages of high compressive strength and stiffness. The compound of the elements are connected to each other by steel and concrete, resulting in an element that has all the useful properties of both materials The two main types of composite column are the steel-reinforcement concrete (SRC) column shown in Fig. 1, which consists of a steel section encased in reinforced or unreinforced concrete, and the concrete-filled steel tube (CFT) columns shown in Fig.no 2 consist of concrete filled composite column. CFT columns have many advantages over SRC columns. The major benefits of concrete filled columns are:

*1)* Steel column acts as permanent and integral formwork
*2)* The steel column provides external reinforcement, and
*3)* The steel column support several levels of construction prior to concrete being pumped

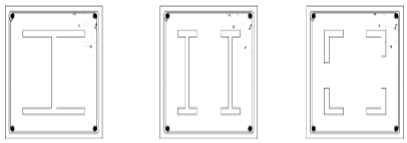

Fig.1: Concrete-encased Composite column

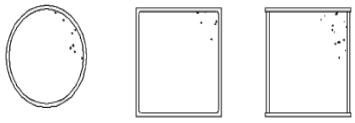

Fig.2: Concrete-filled Composite Column

### *A. Concrete Filled Steel Tube*

The use of CFTS provides great cost savings by increasing the area to be leased, at the same time, the required cross-sectional dimensions. This is particularly important for the design of high-rise buildings in the towns and cities, where the cost of providing the space for rent is a lot higher. It is particularly noticeable in the lower floors of high-rise buildings, which are usually of a short column. CFTs can provide a good monotonicity, and the buildings in the two orthogonal directions. The use of the elements of the composite CFT in every major area of small and medium-sized building with a seismic reduce the time in order to take full advantage of the capabilities in a two-way CFT.

## II. LITERATURE REVIEW

*A. Behavior Of Concrete-Filled Steel Tubes Subjected To Axial Impact Loads (2020)*

The paper presents an experimental investigation of the dynamic behavior of a twelve-square-and rectangular-shaped CFST stub columns subjected to axial shock-loading with a weight testing machine. The study of concrete-filled steel tube elements (CFST) under the static loads are commonly used. However, limited research has been done on the behavior of CFST columns subjected to an axial impact load. At the same time, the moment of the forces, and deformational states of America was in for the shock waves. The models of the last element (FE) has been defined and tested, and with the help of the experimental results and the latest research, the data do not fully account for the effects of the deformation of the steel and the concrete. Then, with the help of a FE model, we study the influence of the cross-sectional shape, the steel strength, concrete compressive strength, steel-to-the-point energy-is the speech, the strike of the dynamic characteristics of CFST contact of the columns.

*B. Flexural Behavior of Circular Concrete Filled Steel Tubes (CFST) Under Sustained Load and Chloride Corrosion*

In this paper, we study the bending behavior of the strength of the concrete and the steel tube (CFST) under long-term loading and chloride corrosion. 7 CFST specimens were tested under four-point bending load. It was found that corrosion will be a noticeable deterioration in the strength in bending, and the ductility of the CFST is in very good condition. In order to determine the full-scale behavior of the CFST under the corrosion of the terms and conditions, a newly-element analysis model analysis was developed. A parametric study was carried out in order to find the most important parameters affecting the residual strength under bending, on the basis of a simplified model for the calculation of the residual strength in the circular bending of the CFST under long-term loading and corrosion have been proposed.

*C. Study on Shear Connectors of Square Concrete Filled Steel Tubes*

The author carried out a study on the intermediate plate (steel ring), and the square CFST. In order to compare the results obtained with the time-tested methods and reviews to FIVE, steel coils CFST. This parameter was the ratio, B/t, the tubes, the number of steel coils, of a thickness of the steel ring, and the distance between the steel rings. The complex column-beam (CFST) filled with concrete, the steel, the pipes, the stress of the beam, the first devoted to the steel in the pipe, and then to the side of the steel tube to the concrete, contacts, link, and the cut, so the CFST cut the contact is a very important part of it. The results of the analysis are in good agreement with the test results, the effect of the length of the two steel rings, and the thickness of the steel rings were studied.

## III.METHODOLOGY

*A. Confinement Effects of Binding Bars*

The confinement effects of binding bars on the behavior of CFT stub columns with binding bars can be summarized in two aspects as follows.

1) *Constraining Lateral Deformation Of Concrete Core:* The interaction among the components of CFT stub column with binding bars is illustrated in Fig. Under the assumption that it is the depth along its longitudinal axis, which is equal to the distance between the longitudinal axes of the connecting bars (bs), which you can get from the Fig. 4 according to the equilibrium of forces as follows

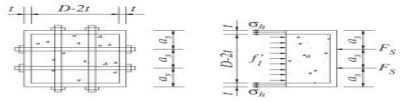


Fig.3: Lateral Confinement Of Concrete

$$f_l' h_s (D - 2t) - \sigma_h h_s . 2t - \left(\frac{D}{a_s} - 1\right) F_s = 0 \quad \text{..... (1)}$$

$$F_s = E_s \varepsilon_s A_s \quad \text{..... (2)}$$

Substituting Eq.(2) into Eq.(1) produces

$$F_l' = \frac{\sigma_h + \frac{D - a_s}{2t} \frac{A_s}{a_s b_s} E_s \varepsilon_s}{\frac{D}{2t} - 1} \quad \text{..... .....(3)}$$

It was observed that the binding bars yielded when the specimens came to ultimate strength. So Eq. (3) can be rewritten as

$$F_l' = \frac{\sigma_h}{\frac{D}{2t} - 1} + \frac{\frac{D - a_s}{2t} \frac{A_s}{a_s b_s} f_y}{\frac{D}{2t} - 1} \quad \text{..... (4)}$$

Where the second part on the right hand side indicates the contribution of binding bars to lateral pressure on concrete, which shows that the lateral confining stress of the concrete core l $F_l'$ increases while the spacing $a_s$ and $b_s$ decreases.

2) *Effect on Local Buckling of Steel Tube:* A local metal bending, steel column, with or without a binding alone is shown in the figure. 5.The concrete in-fill is considered as a rigid medium, restraining the free formation of buckles and forcing them to form away from the concrete. He et al applied an energy formulation to calculate the critical stress in a plate assuming that the displacement is a cosine function. The critical stress is expressed as

$$\sigma_{cr} = k\frac{\pi^2 E_a}{12(1-\mu^2)}\left(\frac{t}{b}\right)^2 \quad \text{..... (5)}$$

Where the buckling parameter k is given by

$$k = \frac{2}{\varphi}\left(\frac{5}{\varphi^2} + 6\varphi^2 + 4\right) \quad \text{..... (6)}$$

$\varphi$ Wavelength parameter defined as

$$\emptyset = \frac{a}{b}$$

It is pointed out that up to half of the wavelength of the local bending, and it is almost the same as the width of the w. Therefore, it is reasonable to assume that a = b, for the specimens without binding bars. Substituting a = b into Eq. (6) But for specimens with binding bars, it can be observed from this experiment that all of the buckling takes place at the spacing between two adjacent rows of level binding bars. It is considered clamped where the rows of level binding bars are located, i.e., a = bs. For specimens with binding bars in this experimental program, bs = D/2 and b = D. apply $bs - \frac{D}{2} and\ b - D$ In eq.(5) calculate results in k

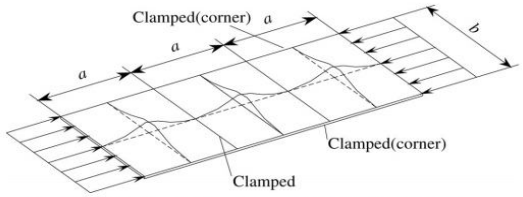

(a) Local buckling for steel plate of CFT column without binding bars.

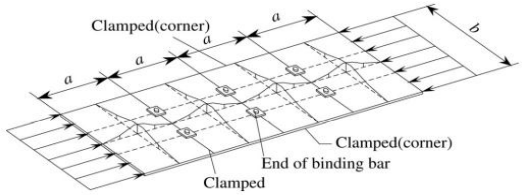

(b) Local buckling for steel plate of CFT column with binding bars.

Fig.4: Local Buckling For Steel Plates of CFT Column

*B. Calculation of Ultimate Strength*

1) *Primary Methods In Current Codes and Specifications :* Methods for calculating the ultimate strength of normal sectioned square CFT stub columns under axial compressive loading are included in many current codes and specifications such as AIJ, EC4, LRFD and GJB4142- 2000. In the limit, the effect of the steel tube on the concrete core, this is ignored in the AIJ, EC4 and LRFD methods. GJB4142 2000, to take account of the importance of the seal of the remarkable endurance of square METERS, the plug of the columns in relation to the casting of the concrete slab and the steel tube column as an entity and taking into account concrete confinement with the so-called constraining factor ξ. The ultimate strength can be expressed as

$$N_u = A_{sc} f_{scy} \quad \text{..... (7)}$$

$$A_{sc} = A_c + A_c \quad \text{..... (8)}$$

$$f_{scy} = (2.212 + B\xi + C\xi^2) fck \quad \text{..... (9)}$$

Where,

$$B - \frac{0.138fy}{235} + 0.7646$$

$$C - \frac{-0.0727\ fck}{20} + 0.0216$$

2) *Model:* It is noted that the methods existing in assume that the steel tube is in a state of uniaxial compressive stress and the concrete obtains its uniaxial ultimate strength while steel yields. Actually the steel tube is subjected to lateral compression after the Poisson's ratio of concrete exceed that of strengthen in the rising loading phase, which leads to the steel tube being in a state of hoop tension and longitudinal compression and the concrete core creature in a triaxial compressive state. The longitudinal compressive strength of the concrete center increases due to such a triaxial compression state. However, the increase in concrete strength outweighs the lessening in the yield strength of steel in vertical compression due to the confinement tension desirable to contain the concrete. The formula for calculating the strength of square CFT stub columns with binding bars are spoken as

$$N_u = A_a f_a + A_c f_{cc} \quad \text{..... (10)}$$

Where,

$f_a$= Longitudinal strength of steel and $f'_{cc}$the longitudinal strength of concrete.

In order to determine$f_{cc}$, the constitutive model of confined concrete proposed by Mander et al. is modified and applied herein. The ultimate in axial strength of confined concrete is known by

$$f_{cc} = f_{ck}\left(-1.254 - 2.254\sqrt{1 + \frac{7.94 f_l}{f_{ck}}} - 2\frac{f_l}{f_{ck}}\right) \quad \text{.. (11)}$$

Where,

$f_l$is equivalent lateral confined stress, given herein by

$$f_l = k_e f_l' \quad \text{..... (12)}$$

In which $f_l'$is calculated from Eq. (4). The confinement effectiveness coefficient ke is divided into ke1, the level confinement effectiveness coefficient, and ke2, the longitudinal confinement coefficient, i.

$$k_e = k_{e1}.k_{e2} \quad \text{..... (13)}$$

Where,

$k_{e1}$ *and* $k_{e2}$ Take the form as

$$k_{e1} - \frac{A_{e1}}{A_{cc1}} \quad \text{..... (14)}$$

$$k_{e2} = \frac{A_{e2}}{A_{cc2}} \quad \text{..... (15)}$$

Where,

$Ae_1$ & $Ae_2$ is the level area of effectively confined concrete along with the longitudinal area of profitability confined concrete core while acting on Acc1 & Acc2 evel area of confined concrete core & longitudinal area of core respectively.

The arching action shown in Fig. 6t is assumed that a 6 will be the second stage of a parabola with a first tangent line at angle$\theta$ So that Ae1 and Acc1 are given by

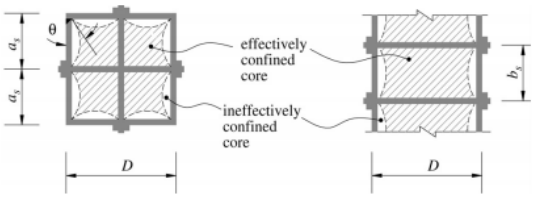


Fig.5: Effectively Concrete Confined Region Square CFT With Binding Bars

$$A_{e1} = (D - 2t)^2 - \sum_{i=1}^{n} \frac{\left[\frac{(D-2t)}{D}\frac{a_s}{}\right]^2 \tan\theta}{6} \quad \text{..... (16)}$$

$$A_{cc1} - (D - 2t)^2 \quad \text{..... (17)}$$

And applying Eqs. (16) and (17) to Eq. (14) produces

$$k_{e1} - \left[1 - \sum_{i=1}^{n} \frac{\left(a_s/D\right)^2 \tan\theta}{6}\right] \quad \text{.....(18)}$$

Similarly it can be deduced that

$$k_{e2} = \left[1 - \frac{b_s \tan\theta}{2(b-2c)}\right]^2 \text{……..…. (19)}$$

Then, from Eq. (13) the confinement effectiveness coefficient is given by

$$k_e = \left[1 - \sum_{i=1}^{n} \frac{\left(c_s/n\right)^2 \tan\theta}{b}\right]\left[1 - \frac{b_s \tan\theta}{2D-2(D-2c)}\right]^2 \text{……..(20)}$$

It is found that the initial tangent angle θ is mainly sensitive to level spacing of binding bars. Base on a linear regression, a simple shape of expression is in employ as

$$\theta - \frac{\pi}{100}\left(13 + \frac{9.2 s_s}{130}\right) \ (rad) \text{…..…. (21)}$$

It is shown that specimens with binding bars failed in postlocal buckling mode. The steel yielded as this category of column reached final strength, hypothetical to obey the Von Mises criteria given by

$$f_a^2 \quad f_a \sigma_h \mid \sigma_h^2 = f_{ay}^2 \text{…….…. (22)}$$

For the local buckling strength of a steel plate fb in CFT columns, Ge and Usami [19] proposed a relationship as

$$\frac{f_b}{f_{ay}} = \frac{1.2}{R} = \frac{0.2}{R^2} \leq 1.0 \text{…….. (23)}$$

This is ensured by keeping R ≥ 0.85; where R is the width–thickness ratio parameter, defined as

$$R = \frac{D}{t}\sqrt{\frac{12(1-\nu^2)}{4\pi^2}}\sqrt{\frac{f_{ay}}{E_a}} \text{……..…. (24)}$$

Then from Eq. (23), the stress states of steel tubes can be determined in the two cases as follows. For R ≥ 0.85 applying fa = fb to Eqs. (23) and (22) results in

$$f_a - \left(\frac{1.2}{R} - \frac{0.2}{R^2}\right) f_{ay} \text{…….. (In Compression) …….. (25)}$$

$$\sigma_h = \frac{f_a - \sqrt{4f_{ay}^2 - 3f_a^2}}{2} \text{…….. (In tension) …….. (26)}$$

For R < 0.85, the effects of local buckling can be ignored [19]. Sakino et al. [20] deduced a relationship between stress coefficient au and bu, which represent hoop stress to yield strength of steel ratio and longitudinal stress to yield strength of steel ratio respectively, based on a large number of results of experiments for circular CFT short columns. The value of coefficients au and bu given as −0.19 and 0.89 respectively are adopted herein to assume the value of hoop stress and longitudinal stress for steel in the case of R < 0.85. Therefore, σh and fa are expressed as follow

$\sigma_h = 0.19\, fay$……(In tension)…….(27)

$$f_a = 0.89\, f_{ay} \text{…….. (In Compression) …….. (28)}$$

3) *Simplification of the Method Proposed :* The method presented above is somewhat complicated and a simplification is proposed below

$$N_u = \emptyset_1 f_{ay} A_c + \emptyset_2 fck\, A_c \text{..... (29)}$$

Where,

φ1 and φ2 are the strength coefficient of steel and that of concrete, defined as

$$\emptyset_1 = \frac{f_a}{f_{ay}}, \qquad \emptyset_2 = \frac{f_{ce}}{f_{ck}} \text{……..…(30)}$$

Based on regression from this program is show fig
. 12, φ1 is given as

$$\emptyset_1 = \begin{cases} 0.09 & R < 0.05 \\ 0.897^{-0.7407} & R > 0.85 \end{cases} \text{.... (31)}$$

It is found that the uniaxial strength of concrete filled in a square steel tube with binding bars primarily depends on the constraining factor of the binding bars ζ and the width-to-thickness ratio parameter R.

$$\emptyset_2 = 1.03R^{-0.0961}(7.3836\zeta + 1.0588) \text{…. (32)}$$

*ISSN: 2321-9653; IC Value: 45.98; SJ Impact Factor: 7.429*
*Volume 9 Issue VI Jun 2021- Available at www.ijraset.com*

*C. Calculation Of Ultimate Bearing Capacity*

In this paper, I have analysed the mechanical behaviour of the reinforcements, which are represented by the effective limit, the coefficient of the concrete. Non-load-bearing capacity is derived based on a unified theory of the strength, in order to analyze the factors that affect the good of the century.

1) *The Unified Theory of the Double-Slip Effect:* Yu Maohong propose a new, unified the income criterion for a double slip, which is based on the income criteria for the double-slip-and-body-double cut block, taking into account the effect of pre-stretching and compression, and the degree of damage to property, under the influence of the principal stress, and its expression is given by equation 1 and equation 2:

$$\begin{cases} F = \sigma_1 - \frac{1}{1+b}(b\sigma_2 + \sigma_3) = \sigma_s & \sigma_2 \le \frac{\sigma_1 + a\sigma_3}{1+a} \\ F' = \frac{1}{1+b}(\sigma_1 + b\sigma_2) - \sigma_3 = \sigma_s & \sigma_2 \ge \frac{\sigma_1 + a\sigma_3}{1+a} \end{cases} \quad \text{..... (1)}$$

$$a = \frac{\sigma_s}{\sigma_c} \qquad b = \frac{2_{\tau_s} - \sigma_s}{\sigma_s \ \tau_s} \text{ ..... (2)}$$

Where,

F and F' = Strength theory function of Principal stress;
σ 1 , σ 2 and σ3 = Principal stress;
σ s , σ c and τ s = Stretching, compression and shear yield stress of material respectively;
B = Degree coefficient of the material fracture influenced by intermediate principal stress;
A =Tension and compression ratio of the material.

2) *Ultimate Bearing Capacity Of Axial Compression:* The cross-section of the concrete filled square steel tubular stiffened is shown in Figure

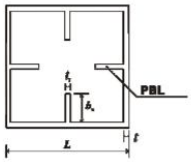


Fig.6: Cross section of Specimen

3) *The Equivalent Transformation Between Square-Circular Concrete Filled Steel Tubular:* There are a large number of experimental studies, which show that the concrete, which is filled by the square steel is a high impact, keeping in a more concrete filled with steel tube, primarily, on their own, to make concrete. This is because, rectangular, steel doesn't have a consistent a binding to the underlying concrete. The installed pipe, the wall shear connectors, the more anchor points, then the local bending can be prevented by effectively and efficiently. In this case, the applications of effective, practical barrier, the coefficient, differential stress, create a level playing field for the thrill. The process in which the equation by 3:

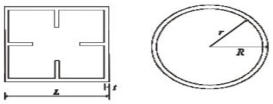

Fig.7: Equivalent Section

$$\begin{cases} L^2 - \pi R^2 \\ (L - 2t)^2 = \pi R^2 \\ r - (L - 2t)/\sqrt{\pi} \\ t' = 2t/\sqrt{\pi} \end{cases} \quad \text{.....(3)}$$

Where,

L is side of square steel tube
t is wall thickness of square steel tube
R is outside diameter of equivalent circular steel
r is inside diameter of equivalent circular steel
t is wall thickness of equivalent circular steel

*D. The Effective Constraint Coefficient Of Concrete*

The effective restriction-area and ineffective restriction-area of core-concrete are separated in Figure 3.17

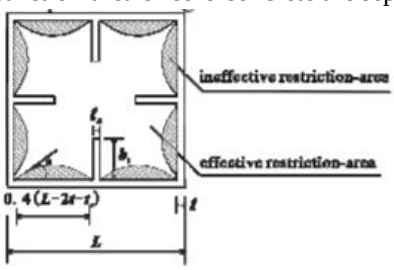


Fig.8: Effective and Ineffective Confined Areas Of Core Concrete

Where $\theta$ is corner cut

$$\tan\theta = \frac{3.6\,t\,f_y}{\left(\frac{L}{t}-t\right)^2}$$

Suppose ineffective restriction area is A1, effective restriction area is As, concrete area is

$$A_C = (L-2t)^2 - 4b_s t_s$$

$$A_s = 8x\,\frac{(0.4(L-2t-r_s))^2 \tan\theta}{s} \quad \ldots\ldots\ldots\ldots\ldots\ldots\ldots\ldots\ldots\ldots \text{(6)}$$

$$A_e = A_c - A_1 \quad \ldots\ldots\ldots\ldots\ldots\ldots\ldots\ldots\ldots\ldots\ldots\ldots\ldots\ldots \text{(7)}$$

Define the effective constraint factor is ke

$$k_e = \frac{A_e}{A_c} = 1 - \frac{A_1}{A_c} = 1 - \frac{1.2\,\tau\,f_y\,(L-2t-r_s)^2}{\left(\frac{L}{2}-t\right)^2\left[(L-2t)^2-4b_s t_s\right]} \quad \ldots\ldots\ldots\ldots\ldots \text{(6)}$$

*E. Binding Effect From Square Steel Tube To Core Concrete*

Reference to literature, assuming square steel force diagram is shown in figure 3.19

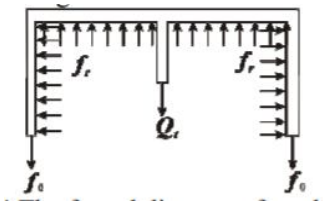


Fig.9: Force Diagram of Steel Tube

Obtained by the mechanical balance

$$2f_\theta tH + nQ_t = f_r(L-2t-t_s) \quad \ldots\ldots\ldots\ldots\ldots\ldots\ldots\ldots\ldots \text{(7)}$$

Where,

H is the height of the steel tube;

n is the number of the holes ;

Qt is the force suffered from shear connectors,

Hu Jianhua suggest that $Q_\tau = 1.95A_s\sqrt{f_c}$

A is area of the stiffener

The results show that, the effect of the shear connectors has related to s b and d ,

When d = bs/2 it work best. So introduce impact factors

$$\gamma = 1 \qquad \frac{|b_s - 2d|}{b_s}$$

$$f_r = \frac{2f_\theta t + \gamma\left(1.95\,n\,A_s\sqrt{fc}\right)/H}{L-2\tau-t_s} \quad \ldots\ldots\ldots\ldots\ldots\ldots\ldots\ldots\ldots\ldots\ldots\ldots\ldots\ldots\ldots\ldots \text{(8)}$$

So the radial stress of the concrete is given by Eq 9

$$f_r^{'} = k_e f_r \quad \ldots\ldots\ldots\ldots\ldots\ldots\ldots\ldots\ldots\ldots\ldots\ldots\ldots\ldots\ldots\ldots\ldots\ldots \text{(9)}$$

*F. Bearing Capacity of Core Concrete*

Core concrete is in three-dimensional stress state, so $0 > \sigma_1 = \sigma_2 > \sigma_3$ , suppose $\sigma_1 = \sigma_2 = f_r^{'}$ , we can get the axial compressive stress of the core concrete from the unified strength theory

$$\sigma_3 = f_c + k\sigma_1 \quad \text{..... (10)}$$

Where σ3 is axial compressive stress of concrete; fc is compressive strength of concrete prism; $k = (1+\sin\varphi)/(1-\sin\varphi)$, k changes between 1.0 to 7.0

Axial compressive strength of effectively confined concrete is taken eq 11

$$f_{ce} = f_c + kf_r^{'} \quad \text{..... (11)}$$

So the carrying capacity of effectively confined concrete is given by Eq. 12

$$N_{ce} - A_s f_{ce} - k_e[(L-2t)^2 - 4h_s t_s](f_c + kf_r^{'}) \quad \text{.....(12)}$$

For the non-effectively confined concrete, because of the decline of the constraints, introduce into the concrete strength reduction factor

$$\gamma_u = 1.67D^{-0.112}$$

Where,

D is outside diameter of equivalent circular pipe. Its axial compressive strength is give by Eq.13:

$$f_{cl} - f_c + \gamma_u kf_r^{'} \quad \text{..... (13)}$$

So the carrying capacity of non-effectively confined concrete is give by Eq.14:

$$N_{cl} = A_1 f_{cl} = (1-k_e)[(L-2t)^2 - 4b_s t_s](f_c + \gamma_u kf_r^{'}) \quad \text{..... (14)}$$

*G. Ultimate Bearing Capacity Of Concrete Filled Stiffened Square Steel Tubular Short Column*

The axial bearing capacity of square concrete-filled steel tubular stub column with PBL was constitutive of the bearing capacity of square steel tube, PBL stiffeners and core concrete, given by Eq.15:

$$N = A_s f_y + N_{ce} + N_{cl} \quad \text{..... (15)}$$

Where As is area of the square steel tube and the PBL stiffeners. Because there are openings on PBL stiffeners, the carrying capacity will be reduced, so introduce into the bearing capacity reduction factor

$$\gamma_s = \left(1 - \frac{d}{b_s}\right)$$

Where, d is the hole diameter, bs is height of rib So,

$$A_s = 4\left[t(L-t) + \left(1 - \frac{d}{b_s}\right)t_s b_s\right]$$

Finally, the axial bearing capacity of square concrete-filled steel tubular stub column is given by Eq. 16:

$$N = 4\left[t(L \quad t) + \left(1 \quad \frac{d}{b_s}\right)t_s b_s\right] + [(L \quad 2t)^2 \quad 4b_s t_s](f_c + kf_r^{'}[\gamma_u + k_e(1 \quad \gamma_u)]] \quad \text{..... (16)}$$

International Journal for Research in Applied Science & Engineering Technology (IJRASET)
*ISSN: 2321-9653; IC Value: 45.98; SJ Impact Factor: 7.429*
*Volume 9 Issue VI Jun 2021- Available at www.ijraset.com*

## IV. RESULT AND DISCUSSION

### A. *Effect of Stiffening Scheme*

#### 1) *Effect of L/B*

Table 1: Load Carrying Capacity of Square Column

| Sr. No | Specimen (mm) | Size of Square (mm) | | Length (mm) | L/B | Space of Binding Arrangement (mm) | | | Size of Stiffener (mm) | | Predicted ultimate strength (KN) | % Error | Load Carrying Capacity by ABAQUS (KN) | % Error |
|---|---|---|---|---|---|---|---|---|---|---|---|---|---|---|
| | | B | t | L | | as | bs | ts | hs | ts | Nuc | | | |
| 1 | US 1 | 80 | 5 | 650 | 8.125 | | | | | | 333.75 | | 353.51 | |
| 2 | SSOS 2 | 80 | 5 | 650 | 8.125 | 40 | 650 | 5 | 5 | 5 | 483.48 | 30.97 | 440.42 | 19.73 |
| 3 | SSOS 3 | 80 | 5 | 650 | 8.125 | 40 | 650 | 5 | 10 | 5 | 512.87 | 5.73 | 522.26 | 15.67 |
| 4 | SSOS 4 | 80 | 5 | 650 | 8.125 | 40 | 650 | 5 | 15 | 5 | 541.85 | 5.35 | 567.13 | 7.91 |
| 5 | SSES 5 | 80 | 5 | 650 | 8.125 | 40 | 650 | 5 | 5 | 5 | 512.87 | 5.35 | 463.49 | 18.27 |
| 6 | SSES 6 | 80 | 5 | 650 | 8.125 | 40 | 650 | 5 | 10 | 5 | 570.42 | 10.09 | 583.54 | 20.57 |
| 7 | SSES 7 | 80 | 5 | 650 | 8.125 | 40 | 650 | 5 | 15 | 5 | 626.33 | 8.93 | 651.07 | 10.37 |
| 8 | FSOS 8 | 80 | 5 | 650 | 8.125 | 14 | 650 | 5 | 5 | 5 | 713.66 | 12.24 | 765.88 | 14.99 |
| 9 | FSOS 9 | 80 | 5 | 650 | 8.125 | 14 | 650 | 5 | 10 | 5 | 954.89 | 25.26 | 1010.1 | 24.18 |
| 10 | FSOS 10 | 80 | 5 | 650 | 8.125 | 14 | 650 | 5 | 15 | 5 | 1177.36 | 18.90 | 1202 | 15.97 |
| 11 | QPS 11 | 80 | 5 | 650 | 8.125 | 35 | 650 | 5 | 5 | 5 | 502.47 | 57.32 | 526.74 | 56.18 |
| 12 | QPS 12 | 80 | 5 | 650 | 8.125 | 35 | 650 | 5 | 10 | 5 | 550.20 | 8.68 | 530.24 | 0.66 |
| 13 | QPS 13 | 80 | 5 | 650 | 8.125 | 35 | 650 | 5 | 15 | 5 | 596.88 | 7.82 | 630.42 | 15.89 |
| 14 | SVSES 14 | 80 | 5 | 650 | 8.125 | 40 | 650 | 5 | 5 | 5 | 512.87 | 14.07 | 543.5 | 13.79 |
| 15 | SVSES 15 | 80 | 5 | 650 | 8.125 | 40 | 650 | 5 | 10 | 5 | 570.42 | 10.09 | 592.9 | 8.33 |
| 16 | SVSES 16 | 80 | 5 | 650 | 8.125 | 40 | 650 | 5 | 15 | 5 | 626.33 | 8.93 | 652.19 | 9.09 |
| 17 | ISEC 17 | 80 | 5 | 650 | 8.125 | 28.78 | 650 | 5 | 5 | 5 | 528.23 | 15.66 | 593.14 | 9.05 |
| 18 | ISEC 18 | 80 | 5 | 650 | 8.125 | 28.78 | 650 | 5 | 10 | 5 | 600.49 | 12.03 | 647.06 | 8.33 |
| 19 | ISEC 19 | 80 | 5 | 650 | 8.125 | 28.78 | 650 | 5 | 15 | 5 | 670.47 | 10.44 | 711.77 | 9.09 |
| 20 | US 20 | 80 | 5 | 850 | 10.625 | | | | | | 333.75 | | 347.72 | |
| 21 | SSOS 21 | 80 | 5 | 850 | 10.625 | 40 | 850 | 5 | 5 | 5 | 478.80 | 30.29 | 474.02 | 26.64 |
| 22 | SSOS 22 | 80 | 5 | 850 | 10.625 | 40 | 850 | 5 | 10 | 5 | 503.61 | 4.93 | 507.88 | 6.67 |
| 23 | SSOS 23 | 80 | 5 | 850 | 10.625 | 40 | 850 | 5 | 15 | 5 | 528.10 | 4.64 | 580.65 | 12.53 |
| 24 | SSES 24 | 80 | 5 | 850 | 10.625 | 40 | 850 | 5 | 5 | 5 | 503.61 | 4.64 | 520.17 | 10.42 |
| 25 | SSES 25 | 80 | 5 | 850 | 10.625 | 40 | 850 | 5 | 10 | 5 | 552.27 | 8.81 | 529.62 | 1.78 |
| 26 | SSES 26 | 80 | 5 | 850 | 10.625 | 40 | 850 | 5 | 15 | 5 | 599.68 | 7.91 | 571.2 | 7.28 |
| 27 | FSOS 27 | 80 | 5 | 850 | 10.625 | 14 | 850 | 5 | 5 | 5 | 661.81 | 9.39 | 636.98 | 10.33 |
| 28 | FSOS 28 | 80 | 5 | 850 | 10.625 | 14 | 850 | 5 | 10 | 5 | 855.60 | 22.65 | 828.08 | 23.08 |
| 29 | FSOS 29 | 80 | 5 | 850 | 10.625 | 14 | 850 | 5 | 15 | 5 | 1035.04 | 17.34 | 1035.1 | 20.00 |
| 30 | QPS 30 | 80 | 5 | 850 | 10.625 | 35 | 850 | 5 | 5 | 5 | 494.49 | 52.23 | 510.75 | 50.66 |
| 31 | QPS 31 | 80 | 5 | 850 | 10.625 | 35 | 850 | 5 | 10 | 5 | 534.48 | 7.48 | 586.19 | 12.87 |
| 32 | QPS 32 | 80 | 5 | 850 | 10.625 | 35 | 850 | 5 | 15 | 5 | 573.67 | 6.83 | 585.24 | 0.16 |
| 33 | SVSES 33 | 80 | 5 | 850 | 10.625 | 40 | 850 | 5 | 5 | 5 | 503.61 | 12.21 | 502.2 | 14.19 |
| 34 | SVSES 34 | 80 | 5 | 850 | 10.625 | 40 | 850 | 5 | 10 | 5 | 552.27 | 8.81 | 561.28 | 10.53 |
| 35 | SVSES 35 | 80 | 5 | 850 | 10.625 | 40 | 850 | 5 | 15 | 5 | 599.68 | 7.91 | 596.36 | 5.88 |
| 36 | ISEC 36 | 80 | 5 | 850 | 10.625 | 28.78 | 850 | 5 | 5 | 5 | 515.35 | 14.06 | 535.51 | 10.20 |
| 37 | ISEC 37 | 80 | 5 | 850 | 10.625 | 28.78 | 850 | 5 | 10 | 5 | 575.27 | 10.42 | 571.21 | 6.25 |
| 38 | ISEC 38 | 80 | 5 | 850 | 10.625 | 28.78 | 850 | 5 | 15 | 5 | 633.44 | 9.18 | 639.41 | 10.67 |
| 39 | US 39 | 80 | 5 | 1050 | 13.125 | | | | | | 333.75 | | 382.04 | |
| 40 | SSOS 40 | 80 | 5 | 1050 | 13.125 | 40 | 1050 | 5 | 5 | 5 | 475.90 | 29.87 | 451.08 | 15.31 |
| 41 | SSOS 41 | 80 | 5 | 1050 | 13.125 | 40 | 1050 | 5 | 10 | 5 | 497.87 | 4.41 | 482.75 | 6.56 |
| 42 | SSOS 42 | 80 | 5 | 1050 | 13.125 | 40 | 1050 | 5 | 15 | 5 | 519.58 | 4.18 | 538.52 | 10.36 |
| 43 | SSES 43 | 80 | 5 | 1050 | 13.125 | 40 | 1050 | 5 | 5 | 5 | 497.87 | 4.18 | 424.77 | 21.12 |
| 44 | SSES 44 | 80 | 5 | 1050 | 13.125 | 40 | 1050 | 5 | 10 | 5 | 541.04 | 7.98 | 561.34 | 24.33 |
| 45 | SSES 45 | 80 | 5 | 1050 | 13.125 | 40 | 1050 | 5 | 15 | 5 | 583.19 | 7.23 | 631.34 | 11.09 |
| 46 | FSOS 46 | 80 | 5 | 1050 | 13.125 | 14 | 1050 | 5 | 5 | 5 | 629.71 | 7.39 | 624.08 | 1.15 |
| 47 | FSOS 47 | 80 | 5 | 1050 | 13.125 | 14 | 1050 | 5 | 10 | 5 | 794.13 | 20.70 | 802.38 | 22.22 |
| 48 | FSOS 48 | 80 | 5 | 1050 | 13.125 | 14 | 1050 | 5 | 15 | 5 | 946.94 | 16.14 | 936.11 | 14.29 |
| 49 | QPS 49 | 80 | 5 | 1050 | 13.125 | 35 | 1050 | 5 | 5 | 5 | 489.54 | 48.30 | 454 | 51.50 |
| 50 | QPS 50 | 80 | 5 | 1050 | 13.125 | 35 | 1050 | 5 | 10 | 5 | 524.75 | 6.71 | 512.91 | 11.49 |
| 51 | QPS 51 | 80 | 5 | 1050 | 13.125 | 35 | 1050 | 5 | 15 | 5 | 559.30 | 6.18 | 546.22 | 6.10 |
| 52 | SVSES 52 | 80 | 5 | 1050 | 13.125 | 40 | 1050 | 5 | 5 | 5 | 497.87 | 10.98 | 488.56 | 10.56 |
| 53 | SVSES 53 | 80 | 5 | 1050 | 13.125 | 40 | 1050 | 5 | 10 | 5 | 541.04 | 7.98 | 547.52 | 10.77 |
| 54 | SVSES 54 | 80 | 5 | 1050 | 13.125 | 40 | 1050 | 5 | 15 | 5 | 583.19 | 7.23 | 577.39 | 5.17 |
| 55 | ISEC 55 | 80 | 5 | 1050 | 13.125 | 28.78 | 1050 | 5 | 5 | 5 | 507.37 | 13.00 | 504.01 | 12.71 |
| 56 | ISEC 56 | 80 | 5 | 1050 | 13.125 | 28.78 | 1050 | 5 | 10 | 5 | 559.65 | 9.34 | 556.37 | 9.41 |
| 57 | ISEC 57 | 80 | 5 | 1050 | 13.125 | 28.78 | 1050 | 5 | 15 | 5 | 610.52 | 8.33 | 612.01 | 9.09 |
| **Average Error** | | | | | | | | | | | | **13.48** | | **14.29** |

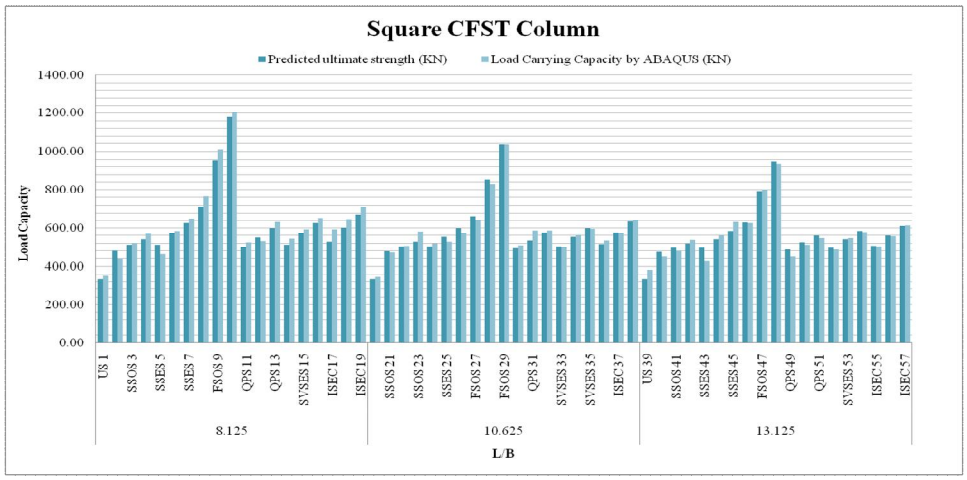


Fig.10: Load Carrying capacity of Square Section

Table 2: Load Carrying Capacity of Rectangular Column

| Sr. No | Specimen (mm) | Size of Square (mm) | | | Length (mm) | L/B | Space of Binding Arrangement (mm) | | | Size of Stiffener (mm) | | Predicted ultimate strength (KN) | % Error | Load Carrying Capacity by ABAQUS (KN) | % Error |
|---|---|---|---|---|---|---|---|---|---|---|---|---|---|---|---|
| | | B | D | t | L | | as | bs | ts | hs | ts | Nuc | | KN | |
| 1 | US 1 | 50 | 100 | 5 | 650 | 13 | | | | | | 311.5 | | 335.25 | |
| 2 | SSES 2 | 50 | 100 | 5 | 650 | 13 | 50 | 650 | 5 | 5 | 5 | 421.17 | 26.04 | 484.68 | 30.83 |
| 3 | SSES 3 | 50 | 100 | 5 | 650 | 13 | 50 | 650 | 5 | 10 | 5 | 442.39 | 4.80 | 489.09 | 0.90 |
| 4 | SSES 4 | 50 | 100 | 5 | 650 | 13 | 50 | 650 | 5 | 15 | 5 | 463.29 | 4.51 | 525.61 | 6.95 |
| 5 | TSOS 5 | 50 | 100 | 5 | 650 | 13 | 41 | 650 | 5 | 5 | 5 | 447.44 | 3.42 | 493.21 | 6.16 |
| 6 | TSOS 6 | 50 | 100 | 5 | 650 | 13 | 41 | 650 | 5 | 10 | 5 | 493.66 | 9.36 | 502.29 | 1.81 |
| 7 | TSOS 7 | 50 | 100 | 5 | 650 | 13 | 41 | 650 | 5 | 15 | 5 | 538.27 | 8.29 | 506.99 | 0.93 |
| 8 | QPS 8 | 50 | 100 | 5 | 650 | 13 | 30 | 650 | 5 | 5 | 5 | 471.89 | 12.33 | 489.00 | 3.55 |
| 9 | QPS 9 | 50 | 100 | 5 | 650 | 13 | 30 | 650 | 5 | 10 | 5 | 540.75 | 12.73 | 569.95 | 14.20 |
| 10 | QPS 10 | 50 | 100 | 5 | 650 | 13 | 30 | 650 | 5 | 15 | 5 | 606.19 | 10.80 | 644.32 | 11.54 |
| 11 | PRS 11 | 50 | 100 | 5 | 650 | 13 | 35 | 650 | 5 | 5 | 5 | 502.99 | 17.02 | 510.36 | 20.79 |
| 12 | PRS 12 | 50 | 100 | 5 | 650 | 13 | 35 | 650 | 5 | 10 | 5 | 598.86 | 16.01 | 589.61 | 13.44 |
| 13 | PRS 13 | 50 | 100 | 5 | 650 | 13 | 35 | 650 | 5 | 15 | 5 | 687.23 | 12.86 | 694.24 | 15.07 |
| 14 | SVSES14 | 50 | 100 | 5 | 650 | 13 | 50 | 650 | 5 | 5 | 5 | 442.39 | 35.63 | 450.37 | 35.13 |
| 15 | SVSES15 | 50 | 100 | 5 | 650 | 13 | 50 | 650 | 5 | 10 | 5 | 483.86 | 8.57 | 502.14 | 10.31 |
| 16 | SVSES16 | 50 | 100 | 5 | 650 | 13 | 50 | 650 | 5 | 15 | 5 | 524.01 | 7.66 | 538.17 | 6.69 |
| 17 | ISEC17 | 50 | 100 | 5 | 650 | 13 | 62.93 | 650 | 5 | 5 | 5 | 437.67 | 16.48 | 449.54 | 16.47 |
| 18 | ISEC18 | 50 | 100 | 5 | 650 | 13 | 62.93 | 650 | 5 | 10 | 5 | 474.69 | 7.80 | 487.36 | 7.76 |
| 19 | ISEC19 | 50 | 100 | 5 | 650 | 13 | 62.93 | 650 | 5 | 15 | 5 | 510.66 | 7.04 | 524.62 | 7.10 |
| 20 | US 20 | 50 | 100 | 5 | 850 | 17 | | | | | | 311.50 | | 394.81 | |
| 21 | SSES 21 | 50 | 100 | 5 | 850 | 17 | 50 | 850 | 5 | 5 | 5 | 418.43 | 25.55 | 432.65 | 8.75 |
| 22 | SSES 22 | 50 | 100 | 5 | 850 | 17 | 50 | 850 | 5 | 10 | 5 | 436.99 | 4.25 | 459.41 | 5.82 |
| 23 | SSES 23 | 50 | 100 | 5 | 850 | 17 | 50 | 850 | 5 | 15 | 5 | 455.30 | 4.02 | 506.02 | 9.21 |
| 24 | TSOS 24 | 50 | 100 | 5 | 850 | 17 | 41 | 850 | 5 | 5 | 5 | 440.84 | 3.17 | 497.48 | 1.69 |
| 25 | TSOS 25 | 50 | 100 | 5 | 850 | 17 | 41 | 850 | 5 | 10 | 5 | 480.85 | 8.32 | 512.64 | 2.96 |
| 26 | TSOS 26 | 50 | 100 | 5 | 850 | 17 | 41 | 850 | 5 | 15 | 5 | 519.63 | 7.46 | 538.63 | 4.83 |
| 27 | QPS 27 | 50 | 100 | 5 | 850 | 17 | 30 | 850 | 5 | 5 | 5 | 460.71 | 11.34 | 464.94 | 13.68 |
| 28 | QPS 28 | 50 | 100 | 5 | 850 | 17 | 30 | 850 | 5 | 10 | 5 | 519.19 | 11.26 | 508.61 | 8.59 |
| 29 | QPS 29 | 50 | 100 | 5 | 850 | 17 | 30 | 850 | 5 | 15 | 5 | 575.05 | 9.71 | 584.02 | 12.91 |

| | | | | | | | | | | | | | | | |
|---|---|---|---|---|---|---|---|---|---|---|---|---|---|---|---|
| 30 | PRS 30 | 50 | 100 | 5 | 850 | 17 | 35 | 850 | 5 | 5 | 5 | 487.98 | 15.14 | 485.30 | 16.90 |
| 31 | PRS 31 | 50 | 100 | 5 | 850 | 17 | 35 | 850 | 5 | 10 | 5 | 570.62 | 14.48 | 562.42 | 13.71 |
| 32 | PRS 32 | 50 | 100 | 5 | 850 | 17 | 35 | 850 | 5 | 15 | 5 | 647.51 | 11.88 | 650.36 | 13.52 |
| 33 | SVSES33 | 50 | 100 | 5 | 850 | 17 | 50 | 850 | 5 | 5 | 5 | 436.99 | 32.51 | 432.47 | 33.50 |
| 34 | SVSES34 | 50 | 100 | 5 | 850 | 17 | 50 | 850 | 5 | 10 | 5 | 473.35 | 7.68 | 484.31 | 10.70 |
| 35 | SVSES35 | 50 | 100 | 5 | 850 | 17 | 50 | 850 | 5 | 15 | 5 | 508.72 | 6.95 | 516.01 | 6.14 |
| 36 | ISEC36 | 50 | 100 | 5 | 850 | 17 | 62.93 | 850 | 5 | 5 | 5 | 433.38 | 14.81 | 425.61 | 17.52 |
| 37 | ISEC37 | 50 | 100 | 5 | 850 | 17 | 62.93 | 850 | 5 | 10 | 5 | 466.34 | 7.07 | 472.78 | 9.98 |
| 38 | ISEC38 | 50 | 100 | 5 | 850 | 17 | 62.93 | 850 | 5 | 15 | 5 | 498.51 | 6.45 | 503.14 | 6.03 |
| 39 | US 39 | 50 | 100 | 5 | 1050 | 21 | | | | | | 311.50 | | 372.16 | |
| 40 | SSES 40 | 50 | 100 | 5 | 1050 | 21 | 50 | 1050 | 5 | 5 | 5 | 416.73 | 25.25 | 446.26 | 16.60 |
| 41 | SSES 41 | 50 | 100 | 5 | 1050 | 21 | 50 | 1050 | 5 | 10 | 5 | 433.64 | 3.90 | 476.14 | 6.28 |
| 42 | SSES 42 | 50 | 100 | 5 | 1050 | 21 | 50 | 1050 | 5 | 15 | 5 | 450.35 | 3.71 | 501.36 | 5.03 |
| 43 | TSOS 43 | 50 | 100 | 5 | 1050 | 21 | 41 | 1050 | 5 | 5 | 5 | 436.76 | 3.02 | 452.51 | 9.74 |
| 44 | TSOS 44 | 50 | 100 | 5 | 1050 | 21 | 41 | 1050 | 5 | 10 | 5 | 472.92 | 7.65 | 475.04 | 4.74 |
| 45 | TSOS 45 | 50 | 100 | 5 | 1050 | 21 | 41 | 1050 | 5 | 15 | 5 | 508.08 | 6.92 | 516.20 | 7.97 |
| 46 | QPS 46 | 50 | 100 | 5 | 1050 | 21 | 30 | 1050 | 5 | 5 | 5 | 453.79 | 10.69 | 450.61 | 12.71 |
| 47 | QPS 47 | 50 | 100 | 5 | 1050 | 21 | 30 | 1050 | 5 | 10 | 5 | 505.84 | 10.29 | 510.69 | 11.76 |
| 48 | QPS 48 | 50 | 100 | 5 | 1050 | 21 | 30 | 1050 | 5 | 15 | 5 | 555.78 | 8.99 | 560.32 | 8.86 |
| 49 | PRS 49 | 50 | 100 | 5 | 1050 | 21 | 35 | 1050 | 5 | 5 | 5 | 478.70 | 13.87 | 482.14 | 13.95 |
| 50 | PRS 50 | 50 | 100 | 5 | 1050 | 21 | 35 | 1050 | 5 | 10 | 5 | 553.13 | 13.46 | 547.34 | 11.91 |
| 51 | PRS 51 | 50 | 100 | 5 | 1050 | 21 | 35 | 1050 | 5 | 15 | 5 | 622.92 | 11.20 | 630.15 | 13.14 |
| 52 | SVSES52 | 50 | 100 | 5 | 1050 | 21 | 50 | 1050 | 5 | 5 | 5 | 433.64 | 30.39 | 419.17 | 33.48 |
| 53 | SVSES53 | 50 | 100 | 5 | 1050 | 21 | 50 | 1050 | 5 | 10 | 5 | 466.85 | 7.11 | 460.36 | 8.95 |
| 54 | SVSES54 | 50 | 100 | 5 | 1050 | 21 | 50 | 1050 | 5 | 15 | 5 | 499.25 | 6.49 | 504.20 | 8.69 |
| 55 | ISEC55 | 50 | 100 | 5 | 1050 | 21 | 62.93 | 1050 | 5 | 5 | 5 | 430.72 | 13.73 | 435.08 | 13.71 |
| 56 | ISEC56 | 50 | 100 | 5 | 1050 | 21 | 62.93 | 1050 | 5 | 10 | 5 | 461.17 | 6.60 | 471.14 | 7.65 |
| 57 | ISEC57 | 50 | 100 | 5 | 1050 | 21 | 62.93 | 1050 | 5 | 15 | 5 | 490.99 | 6.07 | 501.36 | 6.03 |
| Average Error | | | | | | | | | | | | | 11.35 | | 11.25 |

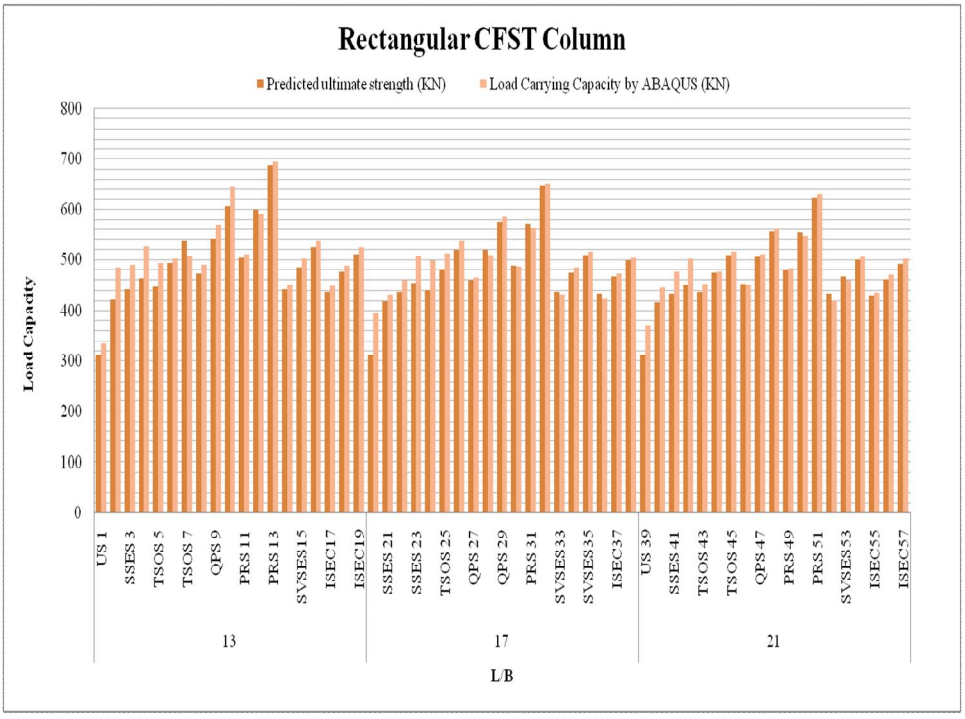


Fig.11: Load Carrying Capacity of Rectangular Section

Table 3: Load Carrying Capacity of Circular Column

| Sr. No | Specimen | Size of Circle (mm) | | Length (mm) | D/L | Space of Binding Arrangement (mm) | | | Size of Stiffener (mm) | | Predicted ultimate strength (KN) | % Error | Load Carrying Capacity by ABAQUS (KN) | % Error |
|---|---|---|---|---|---|---|---|---|---|---|---|---|---|---|
| | | D | t | L | | as | bs | ts | hs | ts | Nu | | KN | |
| 1 | US 1 | 80 | 5 | 650 | 8.125 | | | | | | 261.99 | | 331.61 | |
| 2 | SSOS 2 | 80 | 5 | 650 | 8.125 | 60 | 650 | 5 | 5 | 5 | 396.44 | 33.91 | 428.30 | 22.58 |
| 3 | SSOS 3 | 80 | 5 | 650 | 8.125 | 60 | 650 | 5 | 10 | 5 | 435.64 | 9.00 | 462.14 | 7.32 |
| 4 | SSOS 4 | 80 | 5 | 650 | 8.125 | 60 | 650 | 5 | 15 | 5 | 473.75 | 8.04 | 510.93 | 9.55 |
| 5 | DSEC 5 | 80 | 5 | 650 | 8.125 | 65 | 650 | 5 | 5 | 5 | 432.57 | 8.69 | 507.01 | 0.77 |
| 6 | DSEC 6 | 80 | 5 | 650 | 8.125 | 65 | 650 | 5 | 10 | 5 | 504.96 | 14.34 | 551.35 | 8.04 |
| 7 | DSEC 7 | 80 | 5 | 650 | 8.125 | 65 | 650 | 5 | 15 | 5 | 573.32 | 11.92 | 613.00 | 10.06 |
| 8 | SVSES 8 | 80 | 5 | 650 | 8.125 | 60 | 650 | 5 | 5 | 5 | 396.44 | 30.85 | 399.78 | 34.78 |
| 9 | SVSES 9 | 80 | 5 | 650 | 8.125 | 60 | 650 | 5 | 10 | 5 | 435.64 | 9.00 | 464.13 | 13.86 |
| 10 | SVSES 10 | 80 | 5 | 650 | 8.125 | 60 | 650 | 5 | 15 | 5 | 473.75 | 8.04 | 520.90 | 10.90 |
| 11 | US 11 | 80 | 5 | 850 | 10.625 | | | | | | 261.99 | | 248.08 | |
| 12 | SSOS 12 | 80 | 5 | 850 | 10.625 | 60 | 850 | 5 | 5 | 5 | 391.62 | 33.10 | 387.06 | 35.91 |
| 13 | SSOS 13 | 80 | 5 | 850 | 10.625 | 60 | 850 | 5 | 10 | 5 | 426.25 | 8.13 | 447.07 | 13.42 |
| 14 | SSOS 14 | 80 | 5 | 850 | 10.625 | 60 | 850 | 5 | 15 | 5 | 460.06 | 7.35 | 455.48 | 1.85 |
| 15 | DSEC 15 | 80 | 5 | 850 | 10.625 | 65 | 850 | 5 | 5 | 5 | 423.91 | 7.86 | 450.77 | 1.03 |
| 16 | DSEC 16 | 80 | 5 | 850 | 10.625 | 65 | 850 | 5 | 10 | 5 | 488.58 | 13.24 | 497.36 | 9.37 |
| 17 | DSEC 17 | 80 | 5 | 850 | 10.625 | 65 | 850 | 5 | 15 | 5 | 550.17 | 11.19 | 587.30 | 15.31 |
| 18 | SVSES 18 | 80 | 5 | 850 | 10.625 | 60 | 850 | 5 | 5 | 5 | 391.62 | 28.82 | 417.10 | 28.98 |
| 19 | SVSES 19 | 80 | 5 | 850 | 10.625 | 60 | 850 | 5 | 10 | 5 | 426.25 | 8.13 | 446.28 | 6.54 |
| 20 | SVSES 20 | 80 | 5 | 850 | 10.625 | 60 | 850 | 5 | 15 | 5 | 460.06 | 7.35 | 494.88 | 9.82 |
| 21 | US 21 | 80 | 5 | 1050 | 13.125 | | | | | | 261.99 | | 300.56 | |
| 22 | SSOS 22 | 80 | 5 | 1050 | 13.125 | 60 | 1050 | 5 | 5 | 5 | 388.63 | 32.59 | 366.70 | 18.04 |
| 23 | SSOS 23 | 80 | 5 | 1050 | 13.125 | 60 | 1050 | 5 | 10 | 5 | 420.44 | 7.57 | 489.41 | 25.07 |
| 24 | SSOS 24 | 80 | 5 | 1050 | 13.125 | 60 | 1050 | 5 | 15 | 5 | 451.58 | 6.89 | 452.53 | 7.54 |
| 25 | DSEC 25 | 80 | 5 | 1050 | 13.125 | 65 | 1050 | 5 | 5 | 5 | 418.54 | 7.32 | 402.41 | 11.08 |
| 26 | DSEC 25 | 80 | 5 | 1050 | 13.125 | 65 | 1050 | 5 | 10 | 5 | 478.45 | 12.52 | 466.28 | 13.70 |
| 27 | DSEC 27 | 80 | 5 | 1050 | 13.125 | 65 | 1050 | 5 | 15 | 5 | 535.85 | 10.71 | 545.35 | 14.50 |
| 28 | SVSES 28 | 80 | 5 | 1050 | 13.125 | 60 | 1050 | 5 | 5 | 5 | 388.63 | 27.47 | 409.82 | 24.85 |
| 29 | SVSES 29 | 80 | 5 | 1050 | 13.125 | 60 | 1050 | 5 | 10 | 5 | 420.44 | 7.57 | 437.93 | 6.42 |
| 30 | SVSES 30 | 80 | 5 | 1050 | 13.125 | 60 | 1050 | 5 | 15 | 5 | 451.58 | 6.89 | 457.53 | 4.28 |
| Average Error | | | | | | | | | | | | 14.02 | | 13.54 |

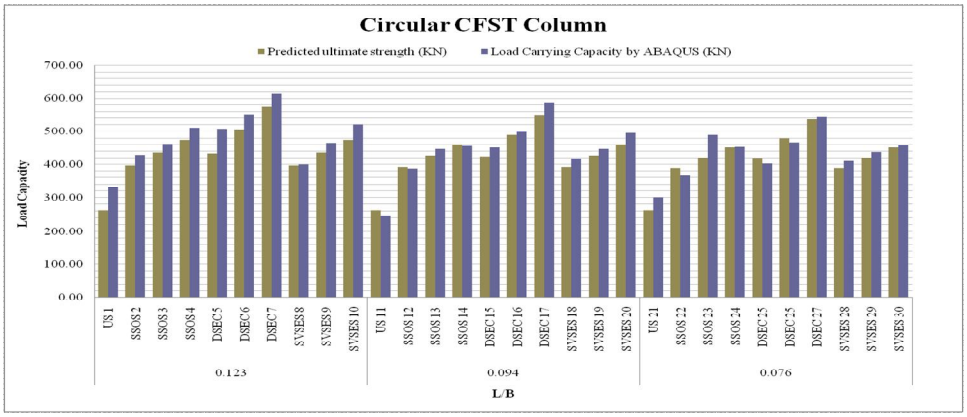


Fig.12: Load Carrying Capacity of Circular Section

*2) Effect of HS/TS*

Table 4: Load Carrying Capacity of Square Column

| Sr. No | Specimen (mm) | Size of Square (mm) | | Length (mm) | Space of Binding Arrangement (mm) | | | Size of Stiffener (mm) | | hs/ts | Predicted ultimate strength (KN) | % Error | Load Carrying Capacity by ABAQUS (KN) | % Error |
|---|---|---|---|---|---|---|---|---|---|---|---|---|---|---|
| | | B | t | L | as | bs | ts | hs | ts | | | | | |
| 1 | SSOS 2 | 80 | 5 | 650 | 40 | 650 | 5 | 5 | 5 | 1 | 483.48 | | 440.42 | |
| 2 | SSES 5 | 80 | 5 | 650 | 40 | 650 | 5 | 5 | 5 | 1 | 512.87 | 5.73 | 463.49 | 4.98 |
| 3 | FSOS 8 | 80 | 5 | 650 | 14 | 650 | 5 | 5 | 5 | 1 | 713.66 | 28.14 | 765.88 | 39.48 |
| 4 | QPS 11 | 80 | 5 | 650 | 35 | 650 | 5 | 5 | 5 | 1 | 502.47 | 29.59 | 526.74 | 31.22 |
| 5 | SVSES 14 | 80 | 5 | 650 | 40 | 650 | 5 | 5 | 5 | 1 | 512.87 | 2.03 | 543.5 | 3.08 |
| 6 | ISEC 17 | 80 | 5 | 650 | 28.78 | 650 | 5 | 5 | 5 | 1 | 528.23 | 2.91 | 593.14 | 8.37 |
| 7 | SSOS 21 | 80 | 5 | 850 | 40.00 | 850 | 5 | 5 | 5 | 1 | 478.80 | 9.36 | 474.02 | 20.08 |
| 8 | SSES 24 | 80 | 5 | 850 | 40 | 850 | 5 | 5 | 5 | 1 | 503.61 | 4.93 | 520.17 | 8.87 |
| 9 | FSOS 27 | 80 | 5 | 850 | 14 | 850 | 5 | 5 | 5 | 1 | 661.81 | 23.90 | 636.98 | 18.34 |
| 10 | QPS 30 | 80 | 5 | 850 | 35 | 850 | 5 | 5 | 5 | 1 | 494.49 | 25.28 | 510.75 | 19.82 |
| 11 | SVSES 33 | 80 | 5 | 850 | 35 | 850 | 5 | 5 | 5 | 1 | 503.61 | 1.81 | 502.2 | 1.67 |
| 12 | ISEC 36 | 80 | 5 | 850 | 28.78 | 850 | 5 | 5 | 5 | 1 | 515.35 | 2.28 | 535.51 | 6.22 |
| 13 | SSOS 40 | 80 | 5 | 1050 | 40 | 1050 | 5 | 5 | 5 | 1 | 475.90 | 7.65 | 451.08 | 15.77 |
| 14 | SSES 43 | 80 | 5 | 1050 | 40 | 1050 | 5 | 5 | 5 | 1 | 497.87 | 4.41 | 424.77 | 5.83 |
| 15 | FSOS 46 | 80 | 5 | 1050 | 14 | 1050 | 5 | 5 | 5 | 1 | 629.71 | 20.94 | 624.08 | 31.94 |
| 16 | QPS 49 | 80 | 5 | 1050 | 35 | 1050 | 5 | 5 | 5 | 1 | 489.54 | 22.26 | 454 | 27.25 |
| 17 | SVSES 52 | 80 | 5 | 1050 | 40 | 1050 | 5 | 5 | 5 | 1 | 497.87 | 1.67 | 488.56 | 7.07 |
| 18 | ISEC 55 | 80 | 5 | 1050 | 28.78 | 1050 | 5 | 5 | 5 | 1 | 507.37 | 1.87 | 504.01 | 3.07 |
| 19 | SSOS 3 | 80 | 5 | 650 | 40 | 650 | 5 | 10 | 5 | 2 | 512.87 | 1.07 | 522.26 | 3.49 |
| 20 | SSES 6 | 80 | 5 | 650 | 40 | 650 | 5 | 10 | 5 | 2 | 570.42 | 10.09 | 583.54 | 10.50 |
| 21 | FSOS 9 | 80 | 5 | 650 | 14 | 650 | 5 | 10 | 5 | 2 | 954.89 | 40.26 | 1010.1 | 42.23 |
| 22 | QPS 12 | 80 | 5 | 650 | 35 | 650 | 5 | 10 | 5 | 2 | 550.20 | 42.38 | 530.24 | 47.51 |
| 23 | SVSES 15 | 80 | 5 | 650 | 40 | 650 | 5 | 10 | 5 | 2 | 570.42 | 3.54 | 592.9 | 10.57 |
| 24 | ISEC 18 | 80 | 5 | 650 | 28.78 | 650 | 5 | 10 | 5 | 2 | 600.49 | 5.01 | 647.06 | 8.37 |
| 25 | SSOS 22 | 80 | 5 | 850 | 40 | 850 | 5 | 10 | 5 | 2 | 503.61 | 16.13 | 507.88 | 21.51 |
| 26 | SSES 25 | 80 | 5 | 850 | 40 | 850 | 5 | 10 | 5 | 2 | 552.27 | 8.81 | 529.62 | 4.10 |
| 27 | FSOS 28 | 80 | 5 | 850 | 14 | 850 | 5 | 10 | 5 | 2 | 855.60 | 35.45 | 828.08 | 36.04 |
| 28 | QPS 31 | 80 | 5 | 850 | 35 | 850 | 5 | 10 | 5 | 2 | 534.48 | 37.53 | 586.19 | 29.21 |
| 29 | SVSES 34 | 80 | 5 | 850 | 40 | 850 | 5 | 10 | 5 | 2 | 552.27 | 3.22 | 561.28 | 4.25 |
| 30 | ISEC 37 | 80 | 5 | 850 | 28.78 | 850 | 5 | 10 | 5 | 2 | 575.27 | 4.00 | 571.21 | 1.74 |
| 31 | SSOS 41 | 80 | 5 | 1050 | 40 | 1050 | 5 | 10 | 5 | 2 | 497.87 | 13.45 | 482.75 | 15.49 |
| 32 | SSES 44 | 80 | 5 | 1050 | 40 | 1050 | 5 | 10 | 5 | 2 | 541.04 | 7.98 | 561.34 | 14.00 |
| 33 | FSOS 47 | 80 | 5 | 1050 | 14 | 1050 | 5 | 10 | 5 | 2 | 794.13 | 31.87 | 802.38 | 30.04 |
| 34 | QPS 50 | 80 | 5 | 1050 | 35 | 1050 | 5 | 10 | 5 | 2 | 524.75 | 33.92 | 512.91 | 36.08 |
| 35 | SVSES 53 | 80 | 5 | 1050 | 40 | 1050 | 5 | 10 | 5 | 2 | 541.04 | 3.01 | 547.52 | 6.32 |
| 36 | ISEC 56 | 80 | 5 | 1050 | 28.78 | 1050 | 5 | 10 | 5 | 2 | 559.65 | 3.33 | 556.37 | 1.59 |
| 37 | SSOS 4 | 80 | 5 | 650 | 40 | 650 | 5 | 15 | 5 | 3 | 541.85 | 3.18 | 567.13 | 1.90 |
| 38 | SSES 7 | 80 | 5 | 650 | 40 | 650 | 5 | 15 | 5 | 3 | 626.33 | 13.49 | 651.07 | 12.89 |
| 39 | FSOS 10 | 80 | 5 | 650 | 14 | 650 | 5 | 15 | 5 | 3 | 1177.36 | 46.80 | 1202 | 45.83 |
| 40 | QPS 13 | 80 | 5 | 650 | 35 | 650 | 5 | 15 | 5 | 3 | 596.88 | 49.30 | 630.42 | 47.55 |
| 41 | SVSES 16 | 80 | 5 | 650 | 40 | 650 | 5 | 15 | 5 | 3 | 626.33 | 4.70 | 652.19 | 3.34 |
| 42 | ISEC 19 | 80 | 5 | 650 | 28.78 | 650 | 5 | 15 | 5 | 3 | 670.47 | 6.58 | 711.77 | 8.37 |
| 43 | SSOS 23 | 80 | 5 | 850 | 40 | 850 | 5 | 15 | 5 | 3 | 528.10 | 21.24 | 580.65 | 18.42 |
| 44 | SSES 26 | 80 | 5 | 850 | 40 | 850 | 5 | 15 | 5 | 3 | 599.68 | 11.94 | 571.2 | 1.63 |
| 45 | FSOS 29 | 80 | 5 | 850 | 14 | 850 | 5 | 15 | 5 | 3 | 1035.04 | 42.06 | 1035.1 | 44.82 |
| 46 | QPS 32 | 80 | 5 | 850 | 35 | 850 | 5 | 15 | 5 | 3 | 573.67 | 44.57 | 585.24 | 43.46 |
| 47 | SVSES 35 | 80 | 5 | 850 | 40 | 850 | 5 | 15 | 5 | 3 | 599.68 | 4.34 | 596.36 | 1.86 |
| 48 | ISEC 38 | 80 | 5 | 850 | 28.78 | 850 | 5 | 15 | 5 | 3 | 633.44 | 5.33 | 639.41 | 6.73 |
| 49 | SSOS 42 | 80 | 5 | 1050 | 40 | 1050 | 5 | 15 | 5 | 3 | 519.58 | 17.98 | 538.52 | 15.78 |
| 50 | SSES 45 | 80 | 5 | 1050 | 40 | 1050 | 5 | 15 | 5 | 3 | 583.19 | 10.91 | 631.34 | 14.70 |
| 51 | FSOS 48 | 80 | 5 | 1050 | 14 | 1050 | 5 | 15 | 5 | 3 | 946.94 | 38.41 | 936.11 | 32.56 |
| 52 | QPS 51 | 80 | 5 | 1050 | 35 | 1050 | 5 | 15 | 5 | 3 | 559.30 | 40.94 | 546.22 | 41.65 |
| 53 | SVSES 54 | 80 | 5 | 1050 | 40 | 1050 | 5 | 15 | 5 | 3 | 583.19 | 4.10 | 577.39 | 5.40 |
| 54 | ISEC 57 | 80 | 5 | 1050 | 28.78 | 1050 | 5 | 15 | 5 | 3 | 610.52 | 4.48 | 612.01 | 5.66 |
| Average Error | | | | | | | | | | | | 16.34 | | 17.52 |

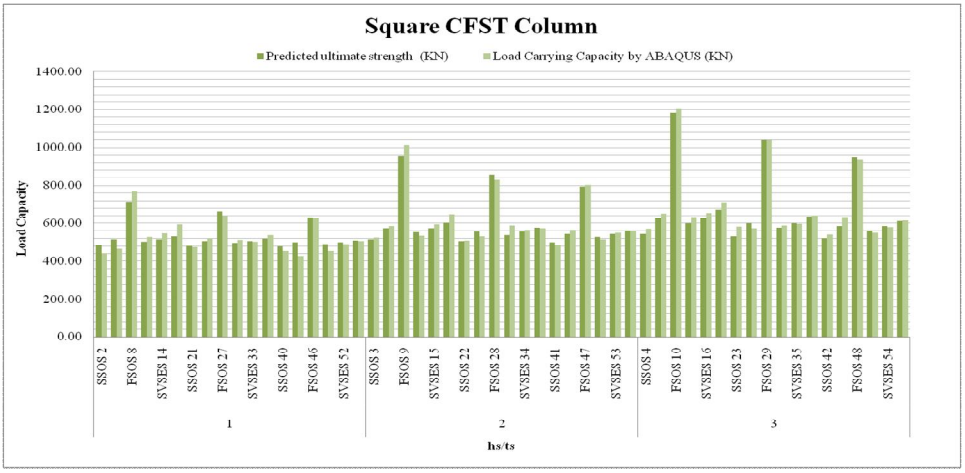


Fig.13: Load Carrying Capacity of Square Column

Table 5: Load Carrying Capacity of Rectangular Column

| Sr. No | Specimen (mm) | Size of Square (mm) | | | Length (mm) | Space of Binding Arrangement (mm) | | | Size of Stiffener (mm) | | hs/ts | Predicted ultimate strength (KN) | % Error | Load Carrying Capacity by ABAQUS (KN) | % Error |
|---|---|---|---|---|---|---|---|---|---|---|---|---|---|---|---|
| | | B | D | t | L | as | bs | ts | hs | ts | | Nuc | | | |
| 1 | SSES 2 | 50 | 100 | 5 | 650 | 50 | 650 | 5 | 5 | 5 | 1 | 421.17 | | 484.68 | |
| 2 | TSOS 5 | 50 | 100 | 5 | 650 | 41 | 650 | 5 | 5 | 5 | 1 | 447.44 | 5.87 | 493.21 | 1.73 |
| 3 | QPS 8 | 50 | 100 | 5 | 650 | 30 | 650 | 5 | 5 | 5 | 1 | 471.89 | 5.18 | 489.00 | 0.85 |
| 4 | PRS 11 | 50 | 100 | 5 | 650 | 35 | 650 | 5 | 5 | 5 | 1 | 502.99 | 6.18 | 510.36 | 4.19 |
| 5 | SVSES14 | 50 | 100 | 5 | 650 | 50 | 650 | 5 | 5 | 5 | 1 | 442.39 | 12.05 | 450.37 | 11.75 |
| 6 | ISEC17 | 50 | 100 | 5 | 650 | 62.93 | 650 | 5 | 5 | 5 | 1 | 437.67 | 1.07 | 449.54 | 0.18 |
| 7 | SSES 21 | 50 | 100 | 5 | 850 | 50 | 850 | 5 | 5 | 5 | 1 | 418.43 | 4.40 | 432.65 | 3.76 |
| 8 | TSOS 24 | 50 | 100 | 5 | 850 | 41 | 850 | 5 | 5 | 5 | 1 | 440.84 | 5.09 | 497.48 | 13.03 |
| 9 | QPS 27 | 50 | 100 | 5 | 850 | 30 | 850 | 5 | 5 | 5 | 1 | 460.71 | 4.31 | 464.94 | 6.54 |
| 10 | PRS 30 | 50 | 100 | 5 | 850 | 35 | 850 | 5 | 5 | 5 | 1 | 487.98 | 5.59 | 485.30 | 4.20 |
| 11 | SVSES33 | 50 | 100 | 5 | 850 | 50 | 850 | 5 | 5 | 5 | 1 | 436.99 | 10.45 | 432.47 | 10.89 |
| 12 | ISEC36 | 50 | 100 | 5 | 850 | 62.93 | 850 | 5 | 5 | 5 | 1 | 433.38 | 0.83 | 425.61 | 1.59 |
| 13 | SSES 40 | 50 | 100 | 5 | 1050 | 50 | 1050 | 5 | 5 | 5 | 1 | 416.73 | 3.84 | 446.26 | 4.63 |
| 14 | TSOS 43 | 50 | 100 | 5 | 1050 | 41 | 1050 | 5 | 5 | 5 | 1 | 436.76 | 4.59 | 452.51 | 1.38 |
| 15 | QPS 46 | 50 | 100 | 5 | 1050 | 30 | 1050 | 5 | 5 | 5 | 1 | 453.79 | 3.75 | 450.61 | 0.42 |
| 16 | PRS 49 | 50 | 100 | 5 | 1050 | 35 | 1050 | 5 | 5 | 5 | 1 | 478.70 | 5.20 | 482.14 | 6.54 |
| 17 | SVSES52 | 50 | 100 | 5 | 1050 | 50 | 1050 | 5 | 5 | 5 | 1 | 433.64 | 9.41 | 419.17 | 13.06 |
| 18 | ISEC55 | 50 | 100 | 5 | 1050 | 62.93 | 1050 | 5 | 5 | 5 | 1 | 430.72 | 0.67 | 435.08 | 3.66 |
| 19 | SSES 3 | 50 | 100 | 5 | 650 | 50 | 650 | 5 | 10 | 5 | 2 | 442.39 | 2.64 | 489.09 | 11.04 |
| 20 | TSOS 6 | 50 | 100 | 5 | 650 | 41 | 650 | 5 | 10 | 5 | 2 | 493.66 | 10.38 | 502.29 | 2.63 |
| 21 | QPS 9 | 50 | 100 | 5 | 650 | 30 | 650 | 5 | 10 | 5 | 2 | 540.75 | 8.71 | 569.95 | 11.87 |
| 22 | PRS 12 | 50 | 100 | 5 | 650 | 35 | 650 | 5 | 10 | 5 | 2 | 598.86 | 9.70 | 589.61 | 3.33 |
| 23 | SVSES15 | 50 | 100 | 5 | 650 | 50 | 650 | 5 | 10 | 5 | 2 | 483.86 | 19.20 | 502.14 | 14.84 |
| 24 | ISEC18 | 50 | 100 | 5 | 650 | 62.93 | 650 | 5 | 10 | 5 | 2 | 474.69 | 1.90 | 487.36 | 2.94 |
| 25 | SSES 22 | 50 | 100 | 5 | 850 | 50 | 850 | 5 | 10 | 5 | 2 | 436.99 | 7.94 | 459.41 | 5.73 |
| 26 | TSOS 25 | 50 | 100 | 5 | 850 | 41 | 850 | 5 | 10 | 5 | 2 | 480.85 | 9.12 | 512.64 | 10.38 |
| 27 | QPS 28 | 50 | 100 | 5 | 850 | 30 | 850 | 5 | 10 | 5 | 2 | 519.19 | 7.38 | 508.61 | 0.79 |
| 28 | PRS 31 | 50 | 100 | 5 | 850 | 35 | 850 | 5 | 10 | 5 | 2 | 570.62 | 9.01 | 562.42 | 9.57 |
| 29 | SVSES34 | 50 | 100 | 5 | 850 | 50 | 850 | 5 | 10 | 5 | 2 | 473.35 | 17.04 | 484.31 | 13.89 |
| 30 | ISEC37 | 50 | 100 | 5 | 850 | 62.93 | 850 | 5 | 10 | 5 | 2 | 466.34 | 1.48 | 472.78 | 2.38 |

| | | | | | | | | | | | | | | | |
|---|---|---|---|---|---|---|---|---|---|---|---|---|---|---|---|
| 31 | SSES 41 | 50 | 100 | 5 | 1050 | 50 | 1050 | 5 | 10 | 5 | 2 | 433.64 | 7.01 | 476.14 | 0.71 |
| 32 | TSOS 44 | 50 | 100 | 5 | 1050 | 41 | 1050 | 5 | 10 | 5 | 2 | 472.92 | 8.31 | 475.04 | 0.23 |
| 33 | QPS 47 | 50 | 100 | 5 | 1050 | 30 | 1050 | 5 | 10 | 5 | 2 | 505.84 | 6.51 | 510.69 | 6.98 |
| 34 | PRS 50 | 50 | 100 | 5 | 1050 | 35 | 1050 | 5 | 10 | 5 | 2 | 553.13 | 8.55 | 547.34 | 6.70 |
| 35 | SVSES53 | 50 | 100 | 5 | 1050 | 50 | 1050 | 5 | 10 | 5 | 2 | 466.85 | 15.60 | 460.36 | 15.89 |
| 36 | ISEC56 | 50 | 100 | 5 | 1050 | 62.93 | 1050 | 5 | 10 | 5 | 2 | 461.17 | 1.22 | 471.14 | 2.29 |
| 37 | SSES 4 | 50 | 100 | 5 | 650 | 50 | 650 | 5 | 15 | 5 | 3 | 463.29 | 0.46 | 525.61 | 10.36 |
| 38 | TSOS 7 | 50 | 100 | 5 | 650 | 41 | 650 | 5 | 15 | 5 | 3 | 538.27 | 13.93 | 506.99 | 3.54 |
| 39 | QPS 10 | 50 | 100 | 5 | 650 | 30 | 650 | 5 | 15 | 5 | 3 | 606.19 | 11.20 | 644.32 | 21.31 |
| 40 | PRS 13 | 50 | 100 | 5 | 650 | 35 | 650 | 5 | 15 | 5 | 3 | 687.23 | 11.79 | 694.24 | 7.19 |
| 41 | SVSES16 | 50 | 100 | 5 | 650 | 50 | 650 | 5 | 15 | 5 | 3 | 524.01 | 23.75 | 538.17 | 22.48 |
| 42 | ISEC19 | 50 | 100 | 5 | 650 | 62.93 | 650 | 5 | 15 | 5 | 3 | 510.66 | 2.55 | 524.62 | 2.52 |
| 43 | SSES 23 | 50 | 100 | 5 | 850 | 50 | 850 | 5 | 15 | 5 | 3 | 455.30 | 10.84 | 506.02 | 3.55 |
| 44 | TSOS 26 | 50 | 100 | 5 | 850 | 41 | 850 | 5 | 15 | 5 | 3 | 519.63 | 12.38 | 538.63 | 6.05 |
| 45 | QPS 29 | 50 | 100 | 5 | 850 | 30 | 850 | 5 | 15 | 5 | 3 | 575.05 | 9.64 | 584.02 | 7.77 |
| 46 | PRS 32 | 50 | 100 | 5 | 850 | 35 | 850 | 5 | 15 | 5 | 3 | 647.51 | 11.19 | 650.36 | 10.20 |
| 47 | SVSES35 | 50 | 100 | 5 | 850 | 50 | 850 | 5 | 15 | 5 | 3 | 508.72 | 21.43 | 516.01 | 20.66 |
| 48 | ISEC38 | 50 | 100 | 5 | 850 | 62.93 | 850 | 5 | 15 | 5 | 3 | 498.51 | 2.01 | 503.14 | 2.49 |
| 49 | SSES 42 | 50 | 100 | 5 | 1050 | 50 | 1050 | 5 | 15 | 5 | 3 | 450.35 | 9.66 | 501.36 | 0.35 |
| 50 | TSOS 45 | 50 | 100 | 5 | 1050 | 41 | 1050 | 5 | 15 | 5 | 3 | 508.08 | 11.36 | 516.20 | 2.87 |
| 51 | QPS 48 | 50 | 100 | 5 | 1050 | 30 | 1050 | 5 | 15 | 5 | 3 | 555.78 | 8.58 | 560.32 | 7.87 |
| 52 | PRS 51 | 50 | 100 | 5 | 1050 | 35 | 1050 | 5 | 15 | 5 | 3 | 622.92 | 10.78 | 630.15 | 11.08 |
| 53 | SVSES54 | 50 | 100 | 5 | 1050 | 50 | 1050 | 5 | 15 | 5 | 3 | 499.25 | 24.77 | 504.20 | 19.99 |
| 54 | ISEC57 | 50 | 100 | 5 | 1050 | 62.93 | 1050 | 5 | 15 | 5 | 3 | 490.99 | 1.68 | 501.36 | 0.56 |
| Average Error | | | | | | | | | | | | | 8.27 | | 7.01 |

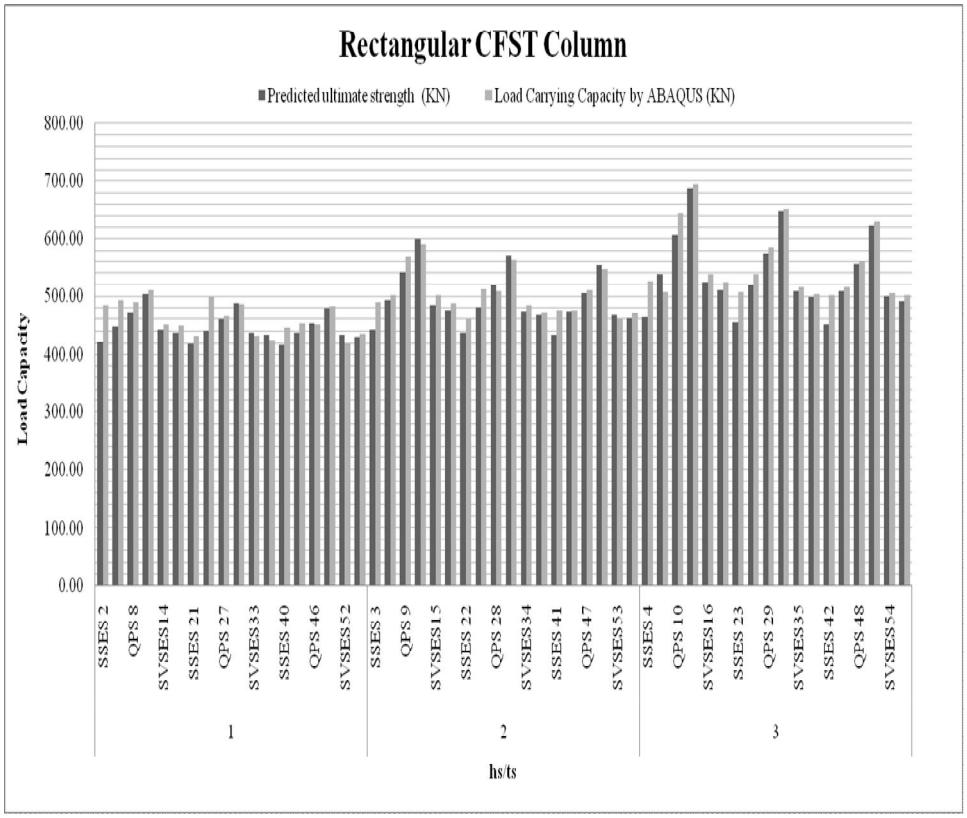


Fig.14: Load Carrying Capacity of Rectangular Column

Table 6: Load Carrying Capacity of Circular Column

| Sr. No | Specimen | Size of Circle (mm) | | Length (mm) | Space of Binding Arrangement (mm) | | | Size of Stiffener (mm) | | h s/ ts | Predicted Ultimate Strength (KN) | % Error | Load Carrying Capacity by ABAQUS (KN) | % Error |
|---|---|---|---|---|---|---|---|---|---|---|---|---|---|---|
| | | D | t | L | as | bs | ts | hs | ts | | Nu | | KN | |
| 1 | SSOS 2 | 80 | 5 | 650 | 60 | 650 | 5 | 5 | 5 | 1 | 396.44 | | 428.3 | |
| 2 | DSEC 5 | 80 | 5 | 650 | 65 | 650 | 5 | 5 | 5 | 1 | 432.57 | 8.35 | 507.01 | 15.52 |
| 3 | SVSES 8 | 80 | 5 | 650 | 60 | 650 | 5 | 5 | 5 | 1 | 396.44 | 8.35 | 399.78 | 21.15 |
| 4 | SSOS 12 | 80 | 5 | 850 | 60 | 850 | 5 | 5 | 5 | 1 | 391.62 | 1.22 | 387.06 | 3.18 |
| 5 | DSEC 15 | 80 | 5 | 850 | 65 | 850 | 5 | 5 | 5 | 1 | 423.91 | 7.62 | 450.77 | 14.13 |
| 6 | SVSES 18 | 80 | 5 | 850 | 60 | 850 | 5 | 5 | 5 | 1 | 391.62 | 7.62 | 417.1 | 7.47 |
| 7 | SSOS 22 | 80 | 5 | 1050 | 60 | 1050 | 5 | 5 | 5 | 1 | 388.63 | 0.76 | 366.7 | 12.08 |
| 8 | DSEC 25 | 80 | 5 | 1050 | 65 | 1050 | 5 | 5 | 5 | 1 | 418.54 | 7.15 | 402.41 | 8.87 |
| 9 | SVSES 28 | 80 | 5 | 1050 | 60 | 1050 | 5 | 5 | 5 | 1 | 388.63 | 7.15 | 409.82 | 1.81 |
| 10 | SSOS 3 | 80 | 5 | 650 | 60 | 650 | 5 | 10 | 5 | 2 | 435.64 | 10.79 | 462.14 | 11.32 |
| 11 | DSEC 6 | 80 | 5 | 650 | 65 | 650 | 5 | 10 | 5 | 2 | 504.96 | 13.73 | 551.35 | 16.18 |
| 12 | SVSES 9 | 80 | 5 | 650 | 60 | 650 | 5 | 10 | 5 | 2 | 435.64 | 13.73 | 464.13 | 15.82 |
| 13 | SSOS 13 | 80 | 5 | 850 | 60 | 850 | 5 | 10 | 5 | 2 | 426.25 | 2.15 | 447.07 | 3.68 |
| 14 | DSEC 16 | 80 | 5 | 850 | 65 | 850 | 5 | 10 | 5 | 2 | 488.58 | 12.76 | 497.36 | 10.11 |
| 15 | SVSES 19 | 80 | 5 | 850 | 60 | 850 | 5 | 10 | 5 | 2 | 426.25 | 12.76 | 446.28 | 10.27 |
| 16 | SSOS 23 | 80 | 5 | 1050 | 60 | 1050 | 5 | 10 | 5 | 2 | 420.44 | 1.36 | 489.41 | 8.81 |
| 17 | DSEC 25 | 80 | 5 | 1050 | 65 | 1050 | 5 | 10 | 5 | 2 | 478.45 | 12.12 | 466.28 | 4.73 |
| 18 | SVSES 29 | 80 | 5 | 1050 | 60 | 1050 | 5 | 10 | 5 | 2 | 420.44 | 12.12 | 437.93 | 6.08 |
| 19 | SSOS 4 | 80 | 5 | 650 | 60 | 650 | 5 | 15 | 5 | 3 | 473.75 | 11.25 | 510.93 | 14.29 |
| 20 | DSEC 7 | 80 | 5 | 650 | 65 | 650 | 5 | 15 | 5 | 3 | 573.32 | 17.37 | 613 | 16.65 |
| 21 | SVSES 10 | 80 | 5 | 650 | 60 | 650 | 5 | 15 | 5 | 3 | 473.75 | 17.37 | 520.9 | 15.02 |
| 22 | SSOS 14 | 80 | 5 | 850 | 60 | 850 | 5 | 15 | 5 | 3 | 460.06 | 2.89 | 455.48 | 12.56 |
| 23 | DSEC 17 | 80 | 5 | 850 | 65 | 850 | 5 | 15 | 5 | 3 | 550.17 | 16.38 | 587.3 | 22.45 |
| 24 | SVSES 20 | 80 | 5 | 850 | 60 | 850 | 5 | 15 | 5 | 3 | 460.06 | 16.38 | 494.88 | 15.74 |
| 25 | SSOS 24 | 80 | 5 | 1050 | 60 | 1050 | 5 | 15 | 5 | 3 | 451.58 | 1.84 | 452.53 | 8.56 |
| 26 | DSEC 27 | 80 | 5 | 1050 | 65 | 1050 | 5 | 15 | 5 | 3 | 535.85 | 15.73 | 545.35 | 17.02 |
| 27 | SVSES 30 | 80 | 5 | 1050 | 60 | 1050 | 5 | 15 | 5 | 3 | 451.58 | 15.73 | 457.53 | 16.10 |
| Average Error | | | | | | | | | | | | 9.79 | | 11.91 |

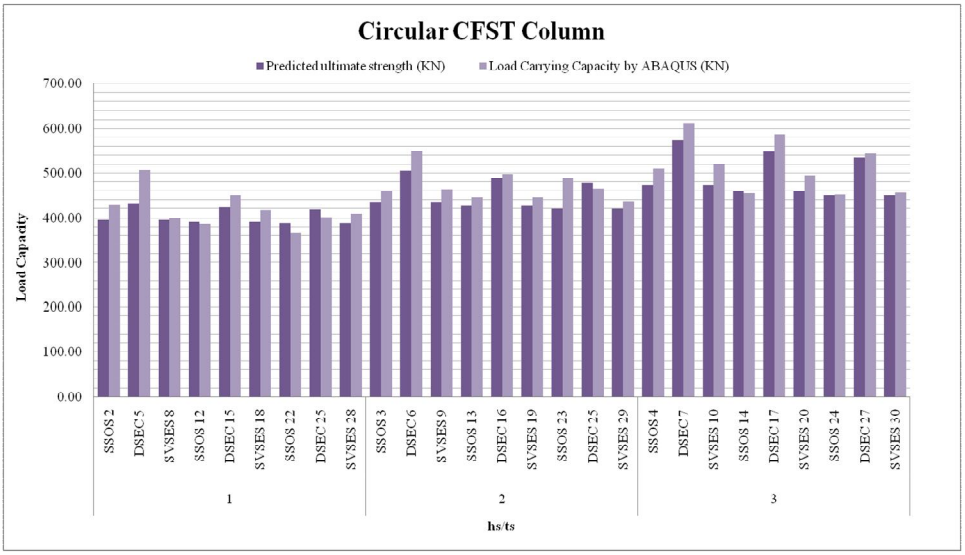


Fig.15: Load Carrying Capacity of Circular Column

## V. CONCLUSIONS

The axial compression 57-square, 57, rectangular, and 30 of circular CFST specimens are conducted. The largest width to thickness ratio reaches 3. Finite element analysis was subsequently carried out to determine the effect of stiffening scheme on the axial load distribution of concrete in steel tube. The following Results are concluded in influence of shear connector.

### *A. Effect of L/B*

*1)* The local buckling appearance of the stiffened columns is relatively different from those of the unstiffened columns. The tube buckling is less pronounced when the number of stiffeners or the stiffener height increases.
*2)* The L/B ratio increase axial load capacity reduces rapidly.
*3)* In this study observed analytical maximum load carrying capacity of 650 mm length four stiffener on opposite side on stiffener size 15x5 mm in square CFST column are 1202 KN as compare to other size of stiffener and length of column.
*4)* In rectangular 650mm length CFST column are maximum load capacity of PBL rib stiffener in 15x5 mm size stiffener is 694.24KN as compare to other.
*5)* In circular 650mm length CFST column are maximum load capacity of double stiffener on each side in 15x5 mm size stiffener is 613 KN as compare to other.
*6)* The Average % error in square, rectangular, circular CFST column is predicted by analytical models is 14.29% 11.25%, 13.54% respectively.

### *B. Effect of hs/ts*

*1)* The maximum axial load increases stably as the stiffener height and the number of stiffeners increase.
*2)* In this study observed analytical maximum load carrying capacity of 650 mm length four stiffener on opposite side on stiffener size 15x5 mm in square CFST column are 1202 KN as compare to other size of stiffener and length of column.
*3)* In rectangular 650mm length CFST column are maximum load capacity of Quarterly placed stiffener in 15x5 mm size stiffener is 644.32 KN as compare to other.
*4)* In circular 650mm length CFST column are maximum load capacity of double stiffener on each side in 15x5 mm size stiffener is 613 KN as compare to other.
*5)* The Average % error in square, rectangular, circular CFST column is predicted by analytical models is 17.52% 7.01%, 11.91% respectively.

### *C. Comparison of Numerical and Analytical Result*

*1)* Using the Numerical results and FEA results through regression analyses, a new model for predicting the axial load capacity is developed for stiffened CFST columns.
*2)* The average ratio of predicting strength to nominal strength of composite column is measured ultimate strength reaches 1.12, 1.02, 1 square, rectangular, circular column respectively.
*3)* Comparison of Average % error in numerical result and analytical result in square, rectangular, circular CFST column is predicted by analytical models is 4% 4.08%, 6.07% respectively.
*4)* The proposed model has low accuracy and the variability in the prediction of the ultimate strength as compared to the existing model.
*5)* Numerical and analytical result results shows good agreement as the % error is within limit less than 10%

## REFERENCES

[1] Aditya Kumar Tiwari, Ashok Kumar Gupta, "Non-Linear, Analysis Of Circular Concrete Filled Steel Tube Columns Under Axial Loading," International Journal of Innovative Technology and Exploring Engineering, Vol. 8, Issue-12, October, 2019.
[2] Akhmet W. Al-Zand Wan Hamidon W. Badaruzaman, et, al, "The Enhanced Performance Of CFST Beams Using Different Strengthening Schemes Involving Unidirectional CFRP Sheets: An Experimental Study ", Engineering Structures, Vol. 128 p. 184-198, 2016.
[3] Chuan-Chuan Hou, Lin-Hai Han, Qing-Li Wang, Chao Hou, "Flexural Behaviour Of Circular Concrete Filled Steel Tubes (CFST) Under Sustained Load And Chloride Corrosion", Thin-Walled Structures, Vol. 107 Pp. 182-196, 2016.
[4] Fareed, Abed, Mohammed Alhamayde et.al, "Experimental And Numerical Investigations Of The Compressive Behaviour Of Concrete Filled Steel Tubes (CFSTs)", Journal of Construction Steel Research, Vol. 80 p. 429-439, 2013.
[5] Georgios Giakoumelis, Dennis Lam, "Axial Capacity Of Circular Concrete-Filled Tube Columns", Journal Of Constructional Steel Research, Vol. 60, Pp. 1049–1068, 2004.
[6] Lin-Hai Han, "The Influence of Concrete Compaction on the Strength of Concrete Filled Steel Tubes", Advances in Structural Engineering, Vol. 3 No. 2 2000.

[7] Qiyun Qiao, Xudong Zhang and Jianhua Hu, “A Study on Shear Connectors of Square Concrete Filled Steel Tubes”, International Journal of Structural and Civil Engineering Research Vol. 4, No. 3, August 2015.
[8] Wei-Wu Qian, Li, Wei, et. al “Analytical Behaviour Of Concrete-Encased CFST Columns Under Cyclic Lateral Loading", Journal of Construction Steel Research, Vol. 120, Pp. 206-220, 2016.
[9] Zhu Yong-Hua Yang, Xiaoqiang Yang, Feixu Sun", "The Behaviour Of Concrete-Filled Steel Tubes Subjected To Axial Impact Loading", Journal of Construction steel Research, Vol. 173, 2020.
[10] Zhi-wu Yu., Fa-xing Ding, C. S. Cai, "Experimental Behaviour Of Circular Concrete-Filled Steel Tube Columns", Journal of structural steel Research, Vol. 63 p. 165-174, 2007.

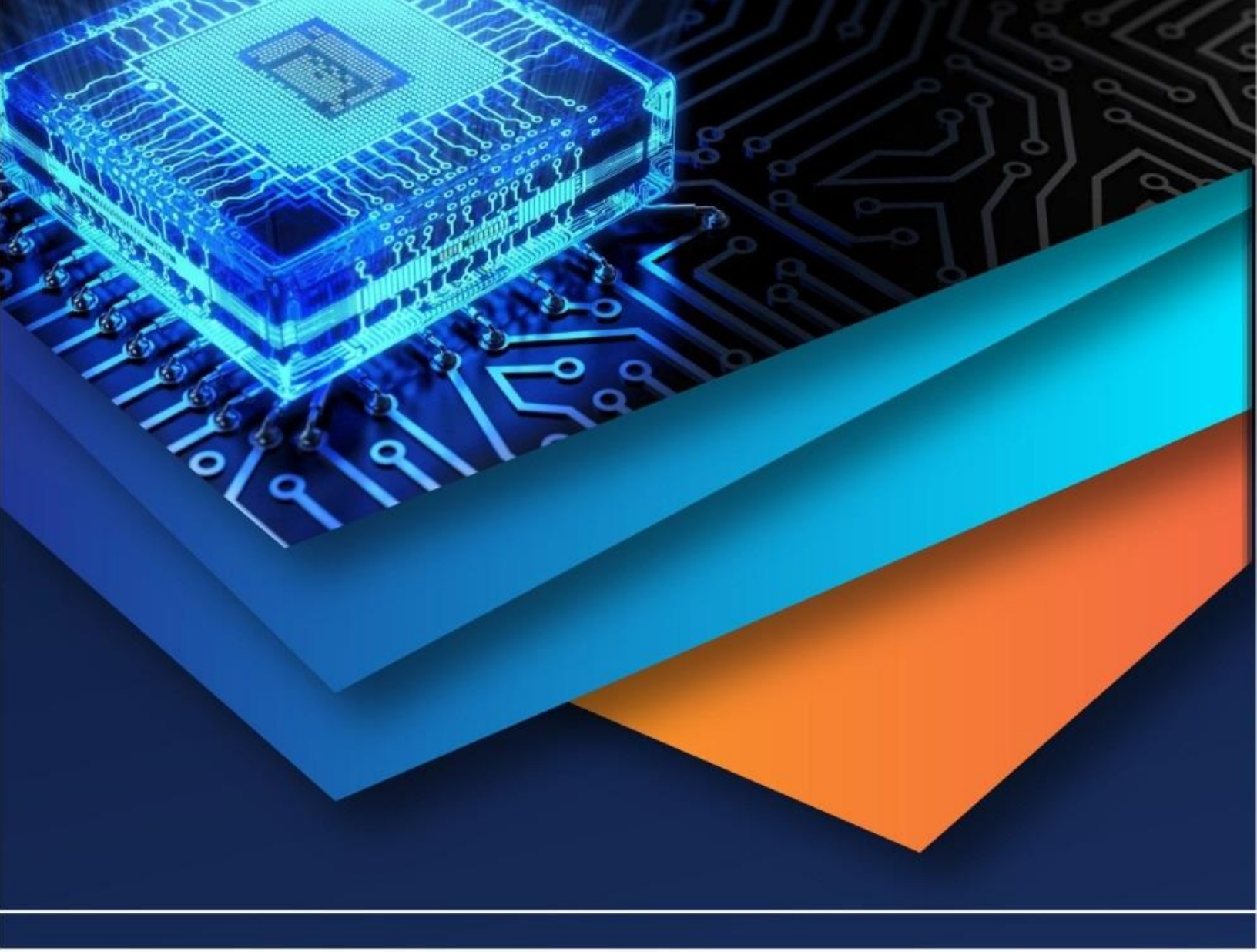

10.22214/IJRASET

45.98

IMPACT FACTOR: 7.129

IMPACT FACTOR: 7.429

# INTERNATIONAL JOURNAL FOR RESEARCH

IN APPLIED SCIENCE & ENGINEERING TECHNOLOGY